Annals of Mathematics and Computer Science ISSN: 2789-7206
Vol 25 (2024) 33-53 https://doi.org/10.56947/amcs.v25.359

STUDY OF MAGNETIC FIELD DEPENDENT VISCOSITY AND TEMPERATURE ON JENKINS MODEL FLUID FLOW OVER A ROTATING DISK

MEGHASHREE G. R.[1], ASHA C. S.[2], SUMANA KRISHNA PRASAD [3], ACHALA L. NARGUND[4], LAXMI RATHOUR[5], VINAY SINGH[6], LAKSHMI NARAYAN MISHRA[7] AND VISHNU NARAYAN MISHRA[8]*

ABSTRACT. The present work involves the study of ferrofluid flow over a stretchable rotating disk maintained at an uniform temperature in the presence of magnetic field dependent viscosity. The system is analyzed through the Jenkins model and the simplified governing equations are represented in the cylindrical co-ordinates. The obtained nonlinear coupled partial differential equations are reduced to a coupled nonlinear ordinary differential equations using the well known Von Karman transformation for rotating disk and solved numerically by the shooting method. The velocity profiles, pressure and temperature are studied by varying the stretching parameter, magnetic field dependent viscosity parameter, material constant, and Prandtl number. The comparison for limiting case of the present problem finds good agreement with the existing literature.

1. INTRODUCTION

The concept of synthesizing fluid for industrial purposes began in the early nineteenth century. Among them, one such fluid is ferrofluid, which is synthesized by dispersing ferro or ferric particles in the base fluid. For a polar base fluid, the model governing the flow consider the body couple and stress couple along with the body force and normal stress, whereas the couple forces are negligible in the case of non-polar base fluid [2, 29]. Here, the dispersed particles are coated with the dispersant in order to avoid agglomeration in the fluid. These fluids are dependent on the applied magnetic field.

Ferrofluid has wide applications, from mechanics to medicine. Ferrofluids are used as lubricants in electro-magnetic power generation, energy harvesting, and as a transformer oil for cooling the system. Further applications involve sealing, magnetic domain detection, and damping. Ferrofluids are used in inclinometers, accelerometers, and nuclear magnetic resonance probes for a specific form of work. In the field of medicine, these fluids are used in magnetic resonance imaging for the evaluation of

Date: Received: Jul 27, 2024; Accepted: Oct 10, 2024.
* Corresponding author.
2010 *Mathematics Subject Classification.* 76D05, 65L06.
Key words and phrases. Ferrofluid, Material constant, Stretching rotating disk, Magnetic field dependent viscosity.

liver, and spleen tumor diagnosis. It is also used for cell separation in the early detection of cancer and as a actuator in the implantation of an artificial heart [14, 21, 39, 50].

Sakiadis [30] was the first to analyze the flow behavior of a fluid past a continuous, constant, moving flat surface. Crane [7] extended the above for the linear stretching sheet. Later, many researchers worked on flow problems over linear, nonlinear and exponential stretching sheet which has its application in fiber technology, process of extrusion, plastic film, polymer sheet production etc. The numerical solution by Tripathy [44] for a micropolar fluid flow over a linear stretching sheet in a porous medium revealed that the magnetic field decreases the velocity distribution. Dulal Pal [19] analyzed the variation in heat and mass transfer due to the presence of buoyancy and thermal radiation parameters over the stretching surface. Abel et al. [1] showed the impact of various parameters on temperature for the cases of prescribed surface temperature and prescribed wall heat flux in the study of boundary layer flow for a viscoelastic fluid with a non-uniform heat source. Siddheshwar et al. [40] analyzed the velocity profiles in radial, transverse, and axial directions in which they showed that the velocity decays with an increase in the viscoelastic parameter and Chandrasekhar number for a magnetohydrodynamic flow past a stretching sheet.

The prolate, oblate, and sphere shapes of particles dispersed in base fluid were considered by Hassan [11] to study the velocity and temperature distribution in the presence of an oscillating magnetic field over a stretchable rotating disk. In which it is mentioned that the prolate shape of the particles had more impact on profiles of velocity and temperature. Ellahi [9] studied the ferrofluid flow over a stretchable rotating disk and noticed that, with an increase in nanoparticle concentration, there is a reduction in the velocity component and enhancement in the temperature. In particular, axial velocity is more impacted by concentration compared to the radial and tangential velocity. Kushal Sharma and Sanjay Kumar [34] showed that heat is enhanced due to the upward movement of a rotating disk in comparison to stationary rotation. Anupam [5] illustrates that the alternating magnetic field with change in the volume concentration of the particles creates resistance in the flow, whereas heat transfer is enhanced in the case of a stationary magnetic field for a flow over a stretchable rotating disk.

Priyadharshini and Karpagam [20] employed machine learning techniques to analyze effective drug delivery in the treatment of cancer through the radiative effects of MHD Williamson bio-fluid. Shamshuddin [33] in his work analyzed the effect of thermal conductivity and variable viscosity on parallel stretching rotating disks. In which he showed the spinning parameter enlarge and shrink the boundary layer of velocity and temperature respectively. Usman et al. [31] in their study analysed entropy generation along with the heat transfer for a fluid over a nonlinear stretching sheet. They revealed that the Brinkman number and porous parameter increase entropy generation, and it gets reduced with increasing material parameter. Adnan et al. [3] considered fluid flow on a bilateral stretching surface with various shapes of nano particles to analyze the velocity profiles and heat transfer. Rana [27] studied the effect of Brownian motion and thermophoresis parameters on a nano fluid flow through a nonlinear stretching sheet. The study shows that an increase in the thermophoresis parameter augments both the temperature and concentration, whereas an increase in the Brownian motion parameter augments the temperature alone. Kalidas [8] analyzed nanofluid flow over a nonlinear stretching sheet with permeability and obtained that velocity reduces and boundary layer thickness increases with an increase in the slip and nonlinear stretching parameters.

Sayantan Sil [41] had explained the impact of constant and varying density of a fluid on a porous medium filled with MHD micropolar fluid. Sandeep et al. [32] considered the permeable stretching sheet for comparative study of non-Newtonian Jeffrey, Maxwell and Oldroyed B nano fluids. Sulochana et al. [42] in the study of Carreau nanofluid flow over a permeable stretching sheet showed that the injection enhances the momentum, thermal, and concentration boundary layers in comparison to the suction. Rajesh Sharma [35] studied the dual solution for a magnetohydrodynamic flow over a stretching/shrinking sheet and showed that the stable results are obtained by increasing the parameters involved in the flow for the first solution and leads to unstable for second set of solution. Paras Ram et al. [12] have studied the magnetic nano fluid flow due to a stretchable rotating plate, in which they showed that the enhancing values of stretching, radiation, viscosity parameters, and Prandtl number reduces the velocity and temperature.

The velocity and temperature shows enhancement and reduction in their profiles by varying parameters like volume fraction of nano particles, radiation, suction parameters, and Reynolds number in the study of heat transfer of nanofluid over a stretching cylinder studied by Shekholeslami et al. [36]. Varun Kumar et al. [48] showed that hybrid nanofluid have a high heat transfer enhancement rate in comparison to nanofluids passed over a linear stretching sheet. The consequences of magnetic and chemical reaction parameters was analysed by Prasannakumara et al. [49] in the study of Casson fluid over a curved surface with a constant stretching. Nandeppanawar et al. [15–17] have analysed heat and mass transfer for various parameters involved in the flow problems over a linear, nonlinear and porous stretching sheet. Paras Ram et al. [26] considers the viscosity to be a function of temperature in which they showed that the stretched parameter reduces the velocity in the radial and axial direction while in contrast, enhance in the tangential direction. Further indicates that temperature shows dual nature with the increase of Prandtl number and stretching parameter after a critical point.

In recent years magnetic field dependent viscosity is studied by many scientists. Magnetic field dependent viscosity in turn known as magneto viscous effect. In this effect when the magnetic field is present, particles in the magnetic fluid form a chain like structures, as a result carrier fluid is made to flow around the chains resulting in increased viscosity. Rosensweig [28] demonstrated experimentally that for a magnetic fluid the magnetoviscous effect takes an exponential form. Further Shliomis [38] provided a theoretical approach and had analysed the negative viscosity effect on the ferrofluid flow. Vaidyanathan [47] to analyse ferrofluid with magneto viscous effect considered the linear form of magnetic viscosity for a small field variation in the form $\eta_B = \eta(1+\vec{\delta}\cdot\vec{B})$. where $\vec{\delta}$ is considered to be isotropic. Further many researchers used the above mentioned form of magnetic field dependent viscosity to analyse ferrofluid flow problems with various geometries.

Ram et al. [22, 23, 25] studied the magnetic field dependent viscosity effect on a ferrofluid flow with rotation, thermal radiation, and porosity parameters. Benard - Marangoni ferroconvection with magnetic field dependent viscosity was discussed by

Nanjundappa et al. [18]. Asha et al. [4] studied the dependence of magneto viscosity on the flow between inclined planes. Sunil et al. [43] analyzed ferro flow with dust particles under the influence of magnetic field dependent viscosity. Thirupathi et al. [45] studied the effect of Magneto - Viscosity of $MnZn$ - ferrite ferrofluid in which they showed that the increase in magnetic field leads to more resistance to the flow, and with further increase, the aggregates of the dispersed materials break down, leading to the free flow of fluid. Sheikholeslami et al. [37] studied the effect of a magnetic source on the heat transfer of a Fe_3O_4 - water based nano fluid and revealed that magnetic source has a reducing and augmenting effect on the velocity and thermal boundary layer thickness respectively. The aforementioned literature survey provides to analyze the present research work for a ferrofluid flow with magnetic field dependent viscosity over a stretching sheet through Jenkins model as it is new to the best of our knowledge. The present paper involves the mathematical formulation of the problem in section 2, the solution methodology in section 3, section 4 include results and discussion, conclusions and graphs are discussed in section 5 and 6.

2. Formulation

The system is studied through the Jenkins model to analyze the steady, axi-symmetric flow of an incompressible ferrofluid over the stretchable rotating disk. The disk is maintained at an uniform temperature and rotates about the vertical axis in a semi-infinite region $z > 0$, where the viscosity of the fluid is subjected to variation in the presence of an applied external magnetic field. The geometry of the flow is as shown in Figure 1 and the governing equations of the system are as follows

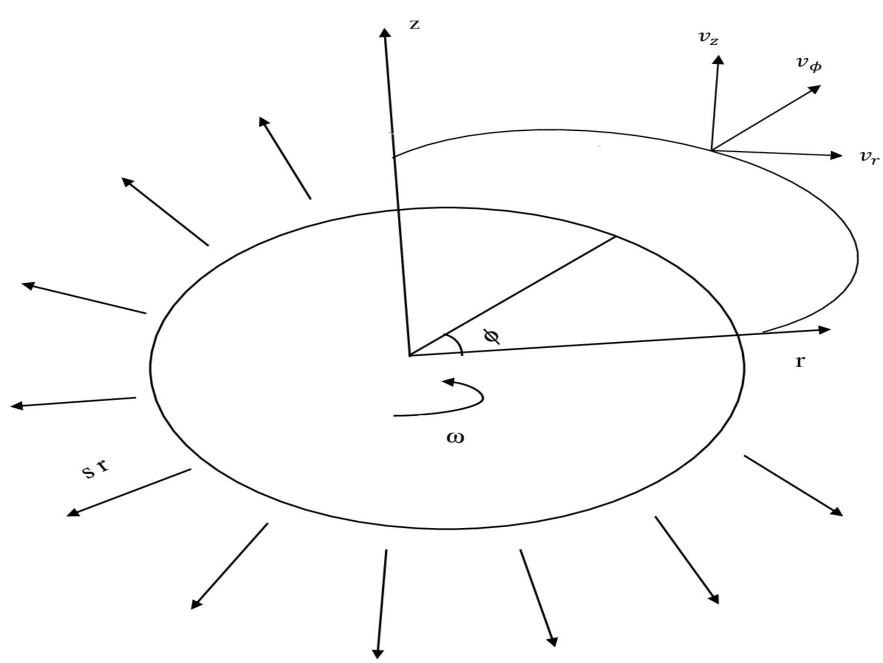

FIGURE 1. Flow configuration of ferrofluid over a stretchable rotating disk

$$\nabla \cdot \vec{q} = 0, \tag{2.1}$$

$$\begin{gathered}\rho\left(\left(\vec{q}\cdot\nabla\right)\vec{q}\right) = -\nabla p + \mu_0\left(\vec{M}\cdot\nabla\right)\vec{H} + \eta_B\nabla^2\vec{q} + \\ \frac{\rho\beta^2}{2}\nabla\times\left(\frac{\vec{M}}{M}\times\left(\nabla\times\vec{q}\right)\times\vec{M}\right),\end{gathered} \tag{2.2}$$

$$\rho C_p\left(\vec{q}\cdot\nabla\right)T = k\nabla^2 T \tag{2.3}$$

$$\nabla\times\vec{H} = 0, \tag{2.4}$$

$$\nabla\cdot(\vec{H} + 4\pi\vec{M}) = 0, \tag{2.5}$$

$$\vec{M} = \overline{\mu}\vec{H} \tag{2.6}$$

$$\vec{M}\times\vec{H} = 0 \tag{2.7}$$

where ρ is the density, $\vec{q}$ is the velocity, p is the pressure, μ_0 is the magnetic permeability, $\vec{M}$ is the magnetization, $\vec{H}$ is the magnetic field, $\eta_B = \eta(1 + \vec{\delta}\cdot\vec{B})$ represents the viscosity dependent on magnetic field, η is the viscosity in the absence of magnetic field, $\vec{\delta}$ is the coefficient of viscosity variation which is isotropic, $\vec{B}$ is the magnetic induction, C_p is the specific heat, T is the temperature, k is the thermal conductivity and $\overline{\mu}$ is the magnetic susceptibility.
Equations (2.1) to (2.7) are represented in the form of cylindrical co-ordinates (r, ϕ, z).

$$\frac{\partial v_r}{\partial r} + \frac{v_r}{r} + \frac{\partial v_z}{\partial z} = 0, \tag{2.8}$$

$$\begin{gathered}-\frac{\partial p}{\partial r} - \frac{H_0\beta^2\overline{\mu}}{2}\left[\frac{\partial^2 v_r}{\partial z^2} - \frac{\partial^2 v_z}{\partial z\partial r}\right] + \eta_B\left[\frac{\partial^2 v_r}{\partial r^2} + \frac{\partial}{\partial r}\left(\frac{v_r}{r}\right) + \frac{\partial^2 v_r}{\partial z^2}\right] \\ = \rho\left[v_r\frac{\partial v_r}{\partial r} + v_z\frac{\partial v_r}{\partial z} - \frac{v_\phi^2}{r}\right],\end{gathered} \tag{2.9}$$

$$\begin{gathered}\frac{H_0\beta^2\overline{\mu}}{2}\left[\frac{\partial^2 v_\phi}{\partial r^2} + \frac{\partial}{\partial r}\left(\frac{v_\phi}{r}\right)\right] + \eta_B\left[\frac{\partial}{\partial r}\left(\frac{v_\phi}{r}\right) + \frac{\partial^2 v_\phi}{\partial r^2} + \frac{\partial^2 v_\phi}{\partial z^2}\right] \\ = \rho\left[v_r\frac{\partial v_\phi}{\partial r} + v_z\frac{\partial v_\phi}{\partial z} + \frac{v_r v_\phi}{r}\right],\end{gathered} \tag{2.10}$$

$$\begin{gathered}-\frac{\partial p}{\partial z} + \frac{\rho H_0\beta^2\overline{\mu}}{2}\left[\left(\frac{\partial^2 v_r}{\partial r\partial z} - \frac{\partial^2 v_z}{\partial r^2}\right) + \frac{1}{r}\left(\frac{\partial v_r}{\partial z} - \frac{\partial v_z}{\partial r}\right)\right] + \\ \eta_B\left[\frac{\partial^2 v_z}{\partial r^2} + \frac{1}{r}\frac{\partial v_z}{\partial r} + \frac{\partial^2 v_z}{\partial z^2}\right] = \rho\left[v_r\frac{\partial v_z}{\partial r} + v_z\frac{\partial v_z}{\partial z}\right],\end{gathered} \tag{2.11}$$

$$\rho C_p\left(v_r\frac{\partial T}{\partial r} + v_z\frac{\partial T}{\partial z}\right) = k\left(\frac{\partial^2 T}{\partial r^2} + \frac{1}{r}\frac{\partial T}{\partial r} + \frac{\partial^2 T}{\partial z^2}\right) \tag{2.12}$$

with initial and boundary conditions for an infinitely large stretching (s) disk and with constant angular velocity (ω) are

$$\begin{cases} v_r = sr, v_\phi = r\omega, v_z = 0, p = p_0, T = T_w & \text{at} \quad z = 0; \\ v_r = v_z = 0, v_z \neq 0, T = T_\infty & \text{as} \quad z = \infty \end{cases} \tag{2.13}$$

Based on the well known Von Karman [13] similarity transformation and Reynolds number the following are the mean flow velocity, pressure and temperature in the form of non dimensional parameter α

$$\begin{aligned} v_r = rsE(\alpha), v_\phi = rsF(\alpha), v_z = \frac{s}{R}G(\alpha), p = \frac{s^2}{R^2}P(\alpha) \\ T - T_\infty = (T_w - T_\infty)\theta(\alpha), \end{aligned} \tag{2.14}$$

where (v_r, v_ϕ, v_z) represents the radial, tangential and axial velocity, $\alpha = z\sqrt{\frac{s}{\nu}}$ the non dimensionless parameter, $R = r\sqrt{\frac{s}{\nu}}$ is the Reynolds number and T_w the uniform temperature.

Equations (2.8) to (2.12) with the boundary conditions as in equation (2.13) owing to equation (2.14) reduce to the set of ordinary nonlinear differential equations with the boundary conditions as follows:

$$G' + 2E = 0, \tag{2.15}$$

$$[m - \overline{\beta}]E'' - E^2 + F^2 - GE' = 0, \tag{2.16}$$

$$mF'' - GF' - 2EF = 0, \tag{2.17}$$

$$P' - mG'' - \overline{\beta}E' + GG' = 0, \tag{2.18}$$

$$\theta'' - PrG\theta' = 0 \tag{2.19}$$

$$\begin{aligned} E(0) = 1, F(0) = \sigma, G(0) = 0, \theta(0) = 1, P(0) = P_0 \\ E(\infty) = 0, F(\infty) = 0, \theta(\infty) = 0, G(\infty) = -c. \end{aligned} \tag{2.20}$$

where m the magnetic field dependent viscosity, $\overline{\beta} = \frac{\rho\beta^2\overline{\mu}H_0}{2\eta}$ represents the material constant, $\sigma = \frac{\omega}{s}$ is a rotation parameter, Pr the Prandtl number and c a non zero number.

3. Solution Methodology

Cochran [6] provided solution to a set of nonlinear differential equations for a flow over a rotating disk in the form of a power series considered as

$$E(\alpha) \approx \sum_{i=1}^{\infty} A_i e^{(-ci\alpha)},$$

$$F(\alpha) \approx \sum_{i=1}^{\infty} B_i e^{(-ci\alpha)},$$

$$G(\alpha) \approx -c + \sum_{i=1}^{\infty} C_i e^{(-ci\alpha)},$$

$$P(\alpha) - P_0 \approx \sum_{i=1}^{\infty} D_i e^{(-ci\alpha)}.$$

In which Cochran specifies the value of $c = 0.886$. Hence we make use of this value of c in our present calculation. Here the set of nonlinear ordinary differential equations (2.15) - (2.19) with the boundary conditions as in equation (2.20) are solved through the shooting method. In the shooting method, the set of higher order ordinary differential equations is reduced to a system of first order differential equations and is solved through fourth order Runge - Kutta method with an initial guess, improvised through the secant method. Here we consider a step size of $h = 0.01$ and an error tolerance value 10^{-6}. Thus obtained numerical solution is depicted through graphs, and reduction of this solution to existing values is shown in Table 6.

3.1. **Skin friction, rate of heat transfer and displacement thickness.** The viscous properties exerts friction for the movement of the fluid above the surface, which is defined as skin friction. The skin friction coefficients for radial and tangential direction are given by

$$C_{fr} = \frac{\tau_r}{\rho v_r^2} \qquad\qquad C_{ft} = \frac{\tau_t}{\rho v_r^2} \tag{3.1}$$

where

$$\tau_r = \left[\eta_B \left(\frac{\partial v_r}{\partial z} + \frac{\partial v_z}{\partial v_r}\right)\right]_{z=0} = \eta m s R E'(0) \tag{3.2}$$

$$\tau_t = \left[\eta_B \left(\frac{\partial v_\phi}{\partial z} + \frac{1}{r}\frac{\partial v_z}{\partial v_\phi}\right)\right]_{z=0} = \eta m s R F'(0) \tag{3.3}$$

By Fourier's law, the rate of heat transfer is given to be

$$q = -\left(k\frac{\partial T}{\partial z}\right)_{z=0} \tag{3.4}$$

Thus the Nusslet number (Nu) is defined as

$$R^{-1}Nu = -\theta'(0)$$

The displacement thickness of the boundary layer for a rotating disk is calculated as

$$d = \frac{1}{r\omega}\int_0^\infty v_\theta dz = \int_0^\infty F(\alpha)d\alpha \tag{3.5}$$

4. Results and Discussion

The graphs are plotted to analyze the effect of magnetic field dependent viscosity (m), rotation parameter (σ), Prandtl number (Pr), and material constant $(\overline{\beta})$ on the fluid flow. Figure 2 represents the profile of radial velocity over a dimensionless parameter α with a varying rotation parameter, which is defined to be the ratio of rotation to stretching. The increasing values of σ indicate that the rotation overcomes the stretching, and as a result, it leads to a larger push of the fluid particles in the radial direction due to the increased centrifugal forces leading to the growth of radial velocity. Moreover at a large distance from the disk, the radial velocity gradually decreases which indicates the effectiveness of centrifugal force is bounded to the vicinage of the disk. Figure 3 represents the gradual increase in the tangential velocity with increase in the rotation parameter.

From Figure 4 we observe that the axial velocity decreases to more and more negative values with increasing parameter of rotation. The negative values implies the fluid particles are drawn towards the disk, which are driven out in radial direction due to increased rotation. Figure 5 represents decreasing profile of pressure, for increasing σ.

Figures $(6-9)$ represent the effect of magnetic field dependent viscosity on the velocity profile, pressure, and temperature. Figure 6 represents the reduction in radial velocity with an increasing magnetic field dependent viscosity parameter, further the velocity profile leads to slower convergence with an increasing values of non dimensionless parameter α. Figure 7 implies that the tangential velocity increases with the magnetic field dependent viscosity parameter. Figure 8 represents variation in the pressure for various values of m. The graph indicates that for an increasing values of m the pressure reduces and reaches a minimum value, further increases and maintains a steady value with increasing α. Figure 9 represents a slight temperature variation with varying m, this slight variation might be prominent in an application problems.

Figures $(10 - 13)$ represents the impact of material constant on velocity profiles, pressure, and temperature. For an increasing $\overline{\beta}$, the profile of the radial velocity initially increases near the disk and further decreases with an increasing α, which leads to faster convergence as shown in Figure 10. It impedes that the boundary layer reduces with an increasing material constant. The tangential velocity in Figure 11 increases with an increasing $\overline{\beta}$, which indicates the material constant enhances the tangential velocity. Figure 12 represents the axial velocity which moves towards the negative region, and the pressure profile in Figure 13 decreases with increasing material constant.

From Figure 14 we can infer that the temperature increases with an increasing $\overline{\beta}$, which ensures the presence of material constant enhance the heat distribution in the fluid. Figure 15 represents variation in the temperature for different Prandtl number. The graph indicates the temperature decreases with an increasing values of Pr, illustrating that the Prandtl number retards the spread of heat in the fluid and there by decreases the temperature of the fluid.

From Table 1 we can extrapolate that the radial skin friction increases with an increase in the stretching parameter and this is by virtue of friction increment at the surface. Further, we notice that the skin friction reduces with an increase in the magnetic field dependent viscosity indicating the magnetic field dependent viscosity reduces the friction of particles adjacent to the surface within the boundary layer. The tangential skin friction values decreases with increase of both the rotating parameter and magnetic field dependent viscosity at the wall as displayed in Table 2.

Table 3 represents the rate of heat transfer for increasing m and σ, calculated values reveal that the heat transfer rate decreases with an increasing m and σ. The impact of Prandtl number on the rate of heat transfer is mentioned in Table 4 which specifies the heat transfer rate decrease with increasing Prandtl number and magnetic field dependent viscosity.

The boundary layer displacement thickness values are depicted in Table 5 for varying values of both the rotating parameter and magnetic field dependent viscosity. From the table, we obtain that the displacement thickness increases with an increasing values of stretching and magnetic field dependent viscosity parameters.

Table 6 explains the comparison of existing literature with our present work for the limiting case. Here with $m = 1$ and the removal of Kelvin body force with a constant viscosity reduces to that of Fang [10], also reduces to the published work of Turkyilmazoglu [46] for $M = 0$. Further with the material constant $\overline{\beta} = 0$ reduces to the work of Paras Ram et al. [24] which finds a good agreement of the present work to above mentioned works for $\sigma = 0$.

5. Conclusion

The present work analysed through Jenkins model provides us to study the effect of magnetic field dependent viscosity, material constant, Prandtl number, and rotation parameter on the system.

- Radial and tangential velocity increase, whereas the axial velocity and pressure move towards the negative region with an increasing values of the rotation parameter.
- The increasing values of the magnetic field dependent viscosity initially reduce the radial velocity near the disk and the reverse process is observed for an increasing values of non dimensionless parameter α, leading to the slower convergence of the profile.
- With the increasing value of material constant, radial velocity and axial velocity reach the steady state faster in comparison to the tangential velocity and temperature.
- The radial and tangential skin friction have opposite behavior in their friction values, with an increase in the rotation parameter.
- There exists reduction in the radial and tangential skin friction values for the increase of magnetic field dependent viscosity parameter.
- Rate of heat transfer decreases with an increase in both the rotation parameter and magnetic field dependent viscosity parameter.
- The Prandtl number has a reducing effect on temperature profiles, which results in reducing the boundary layer thickness.

The present work has application in areas of oceanography, plastic extrusion, rotating machinery lubrication, and so on.

TABLE 1. Radial skin friction with $\overline{\beta_0} = 0.5$

	$\sigma = 2$	$\sigma = 4$	$\sigma = 5$	$\sigma = 7$
m = 1	-0.0819	3.5957	5.9732	11.6152
m = 1.2	-0.1764	3.3978	5.7205	11.2314

TABLE 2. Tangential skin friction with $\overline{\beta_0} = 0.5$

	$\sigma = 2$	$\sigma = 4$	$\sigma = 5$	$\sigma = 7$
m = 1	-3.0457	-7.1764	-9.6020	-15.0694
m = 1.2	-3.3568	-7.8187	-10.4272	-16.3016

TABLE 3. Rate of heat transfer -$\theta'(0)$ with $Pr = 1$ and $\overline{\beta_0} = 0.5$

$-\theta'(0)$	$\sigma = 2$	$\sigma = 4$	$\sigma = 5$	$\sigma = 7$
m = 1	0.8940	1.0728	1.1573	1.3072
m =1.2	0.9273	1.0963	1.1758	1.3228

TABLE 4. Rate of heat transfer -$\theta'(0)$ with $\sigma = 5$ and $\overline{\beta_0} = 0.5$

$-\theta'(0)$	$Pr = 1$	$Pr = 2$	$Pr = 5$	$Pr = 10$
m = 1	1.1573	1.7573	2.8725	4.0544
m = 1.2	1.1758	1.7584	2.5362	3.9943

TABLE 5. Boundary layer displacement thickness $\overline{\beta_0} = 0.5$

	$\sigma = 2$	$\sigma = 4$	$\sigma = 5$	$\sigma = 7$
m = 1	1.2923	2.0938	2.4086	2.9455
m = 1.2	1.3759	2.2680	2.6206	3.2202

TABLE 6. Comparison of the present result with the existing literature results for $m = 1$, $\sigma = 0$, $\overline{\beta_0} = 0$ and $Pr = 1$

	$E'(0)$	$\theta'(0)$
$Fang$	-1.17321000	$-$
$Turkyilmazoglu$	-1.17372073	-0.851991421
$Paras\quad Ram\quad et\quad al.$	-1.17369000	-0.852047000
$Present\quad result$	-1.17377005	-0.852084519

6. GRAPHS

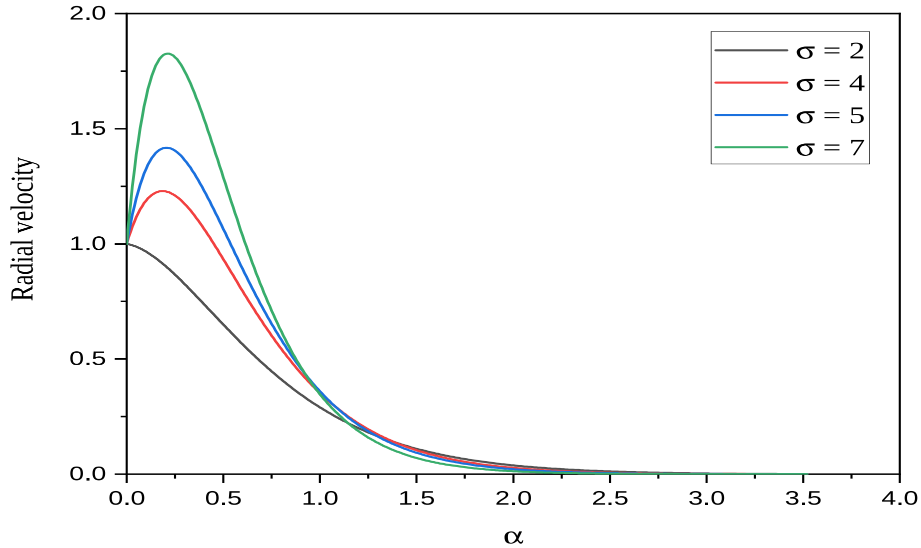

FIGURE 2. Radial velocity versus α for $\overline{\beta} = 0.5$, $m = 1.2$ and $Pr = 1$

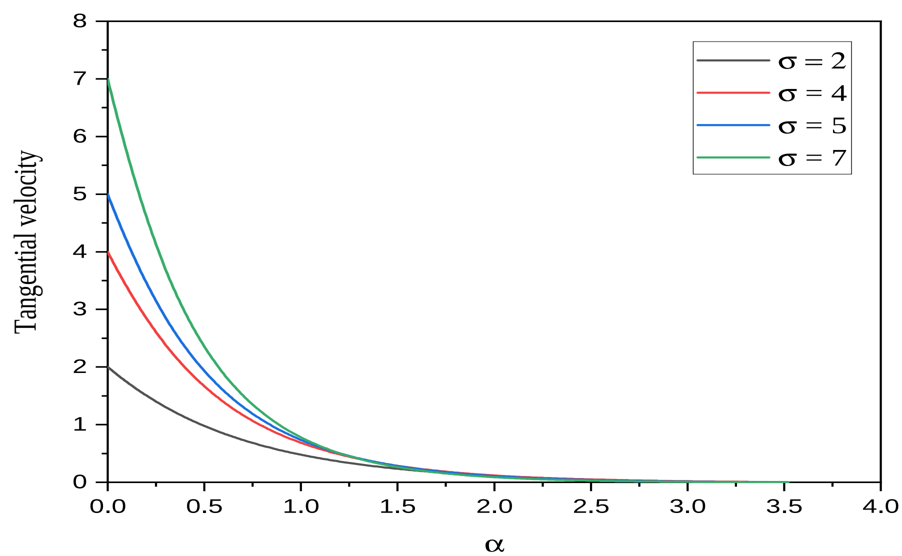

FIGURE 3. Tangential velocity versus α for $\overline{\beta} = 0.5$, $m = 1.2$ and $Pr = 1$

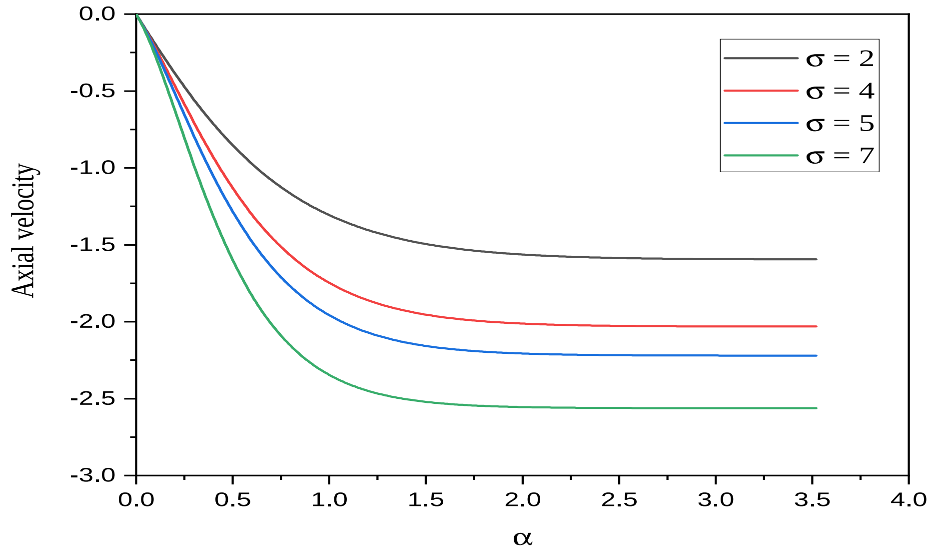

FIGURE 4. Axial velocity versus α for $\overline{\beta} = 0.5$, $m = 1.2$ and $Pr = 1$

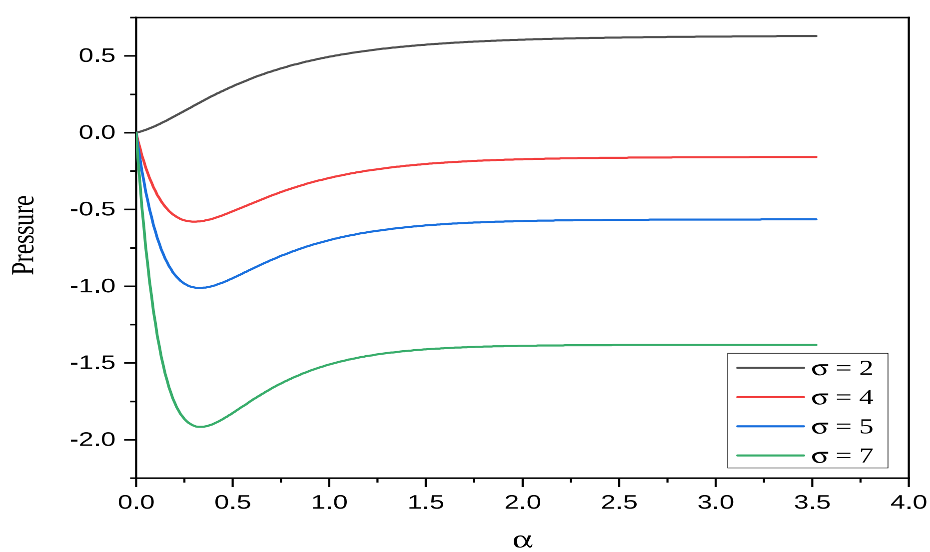

FIGURE 5. Pressure versus versus α for $\overline{\beta} = 0.5$, $m = 1.2$ and $Pr = 1$

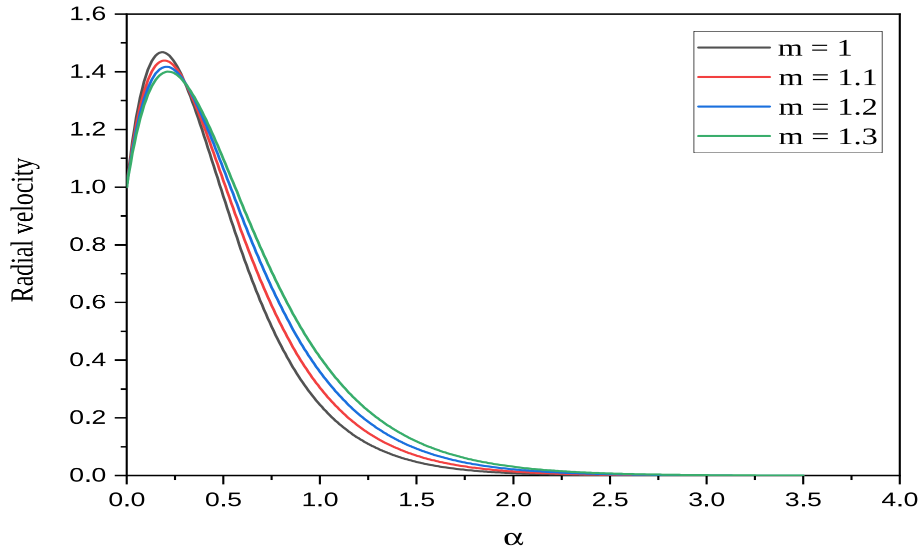

FIGURE 6. Radial velocity versus α for $\overline{\beta} = 0.5$, $Pr = 1$ and $\sigma = 2$

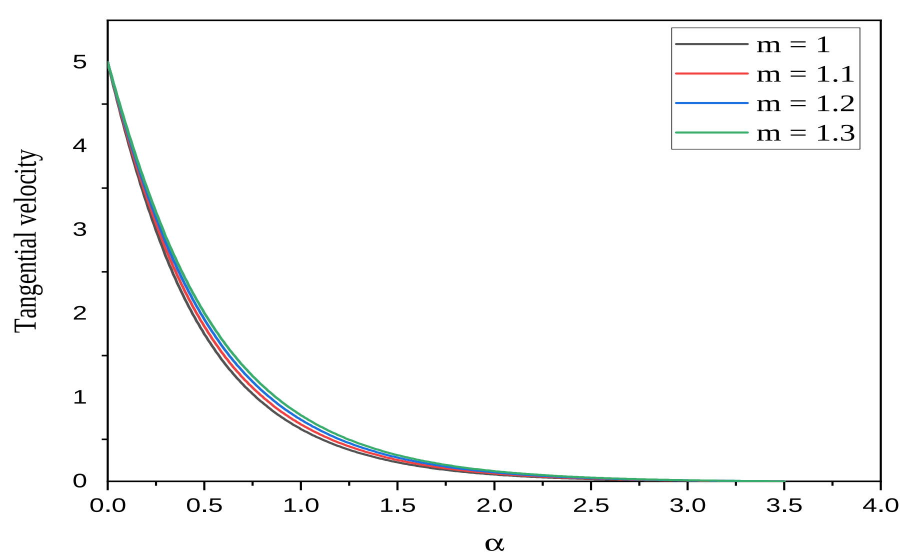

FIGURE 7. Tangential velocity versus α for $\overline{\beta} = 0.5$, $Pr = 1$ and $\sigma = 2$

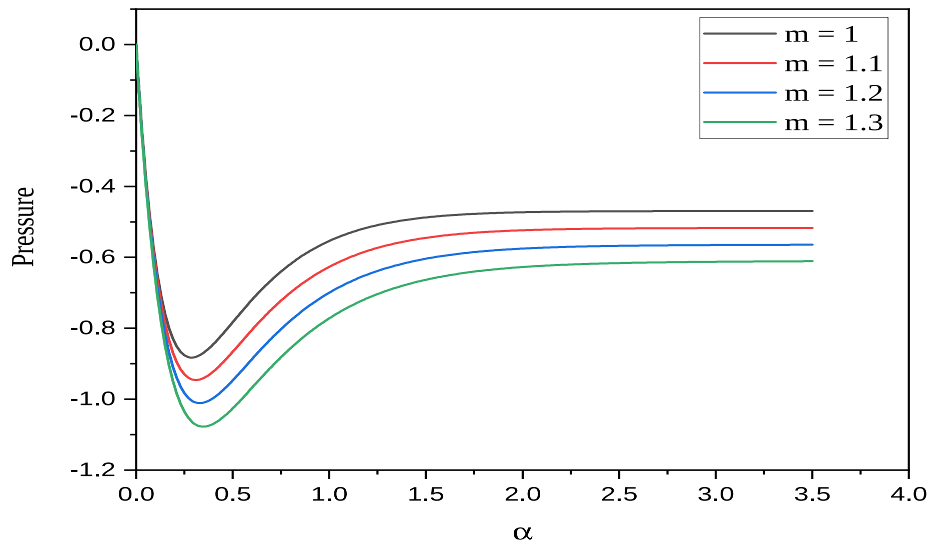

FIGURE 8. Pressure versus α for $\overline{\beta} = 0.5$, $Pr = 1$ and $\sigma = 2$

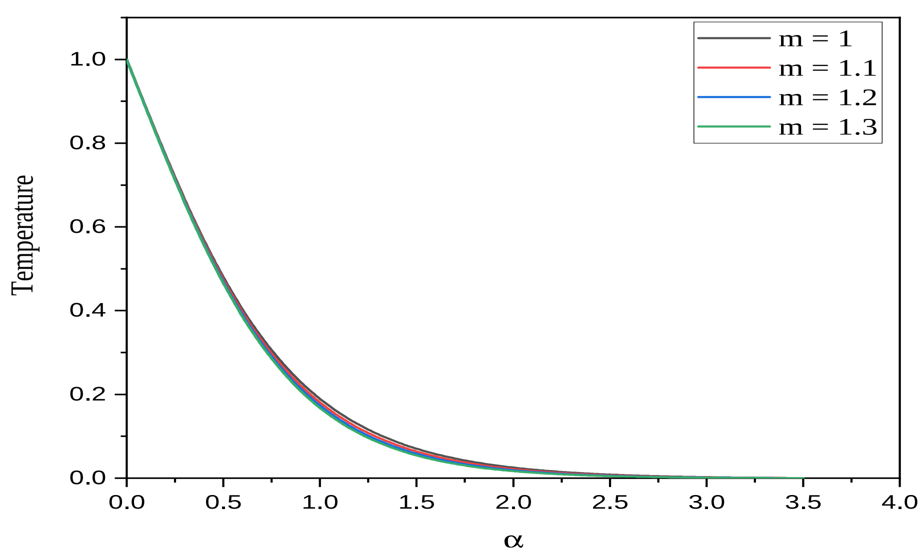

FIGURE 9. Temperature versus α for $\overline{\beta} = 0.5$, $Pr = 1$ and $\sigma = 2$

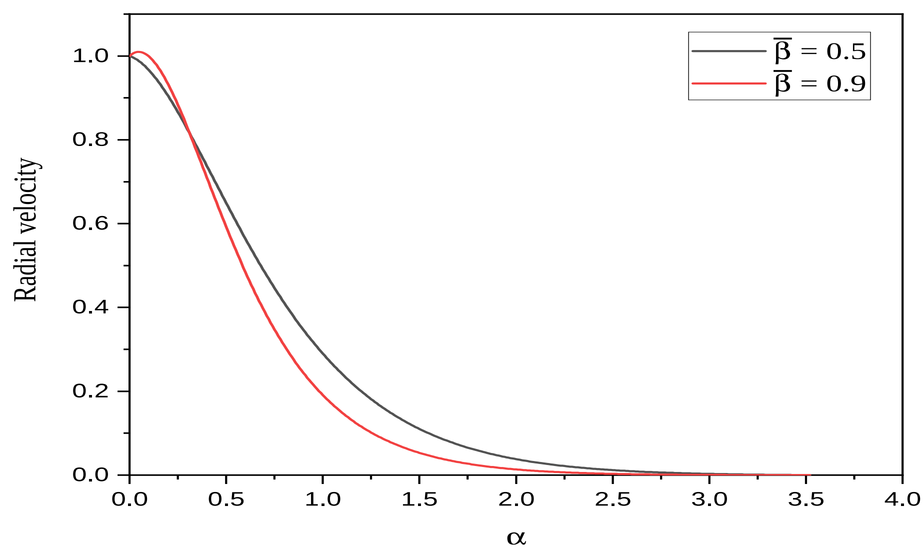

FIGURE 10. Radial velocity versus α for $Pr = 1$, $m = 1.2$ and $\sigma = 2$

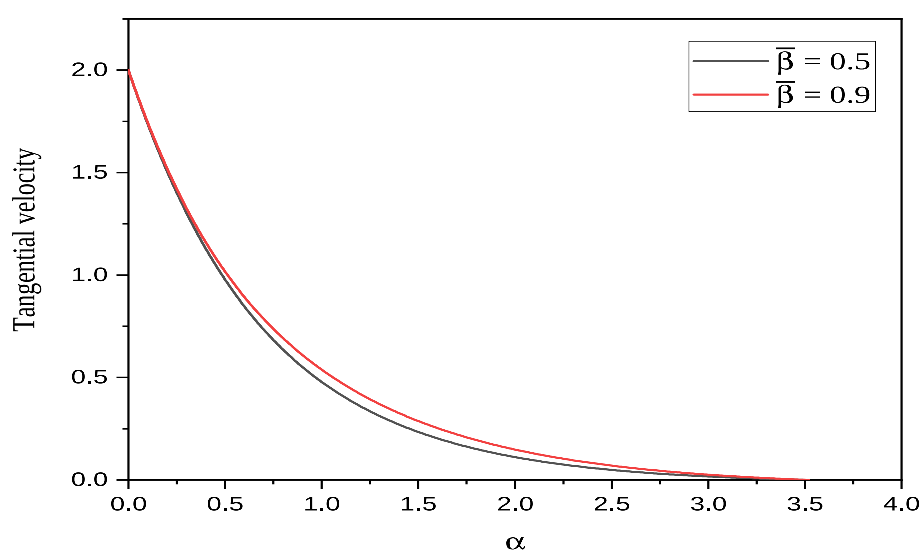

FIGURE 11. Tangential velocity versus α for $Pr = 1$, $m = 1.2$ and $\sigma = 2$

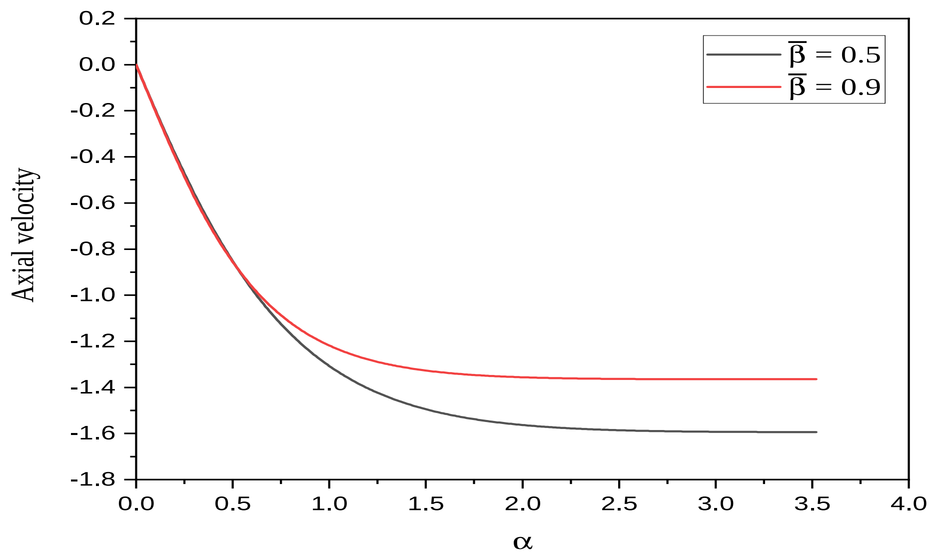

FIGURE 12. Axial velocity versus α for $Pr = 1$, $m = 1.2$ and $\sigma = 2$

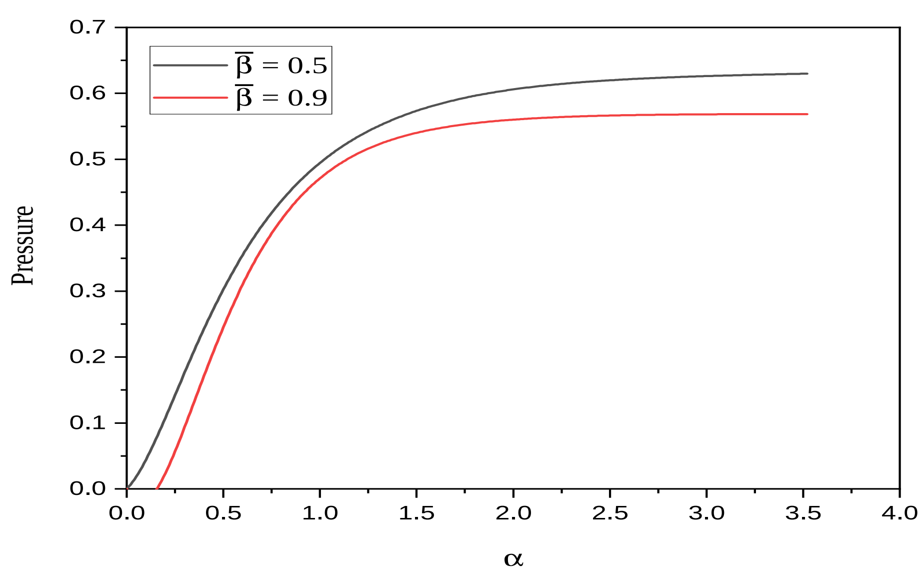

FIGURE 13. Pressure versus α for $Pr = 1$, $m = 1.2$ and $\sigma = 2$

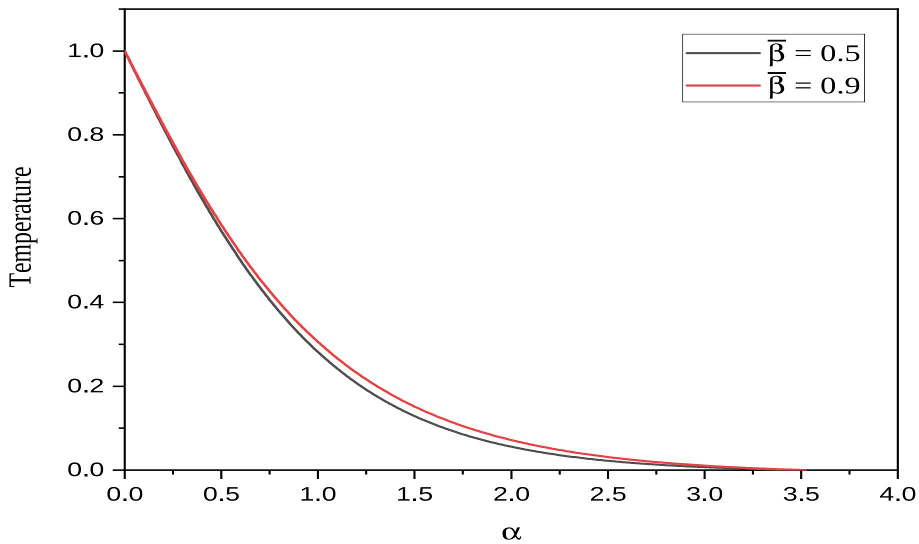

FIGURE 14. Temperature versus α for $Pr = 1$, $m = 1.2$ and $\sigma = 2$

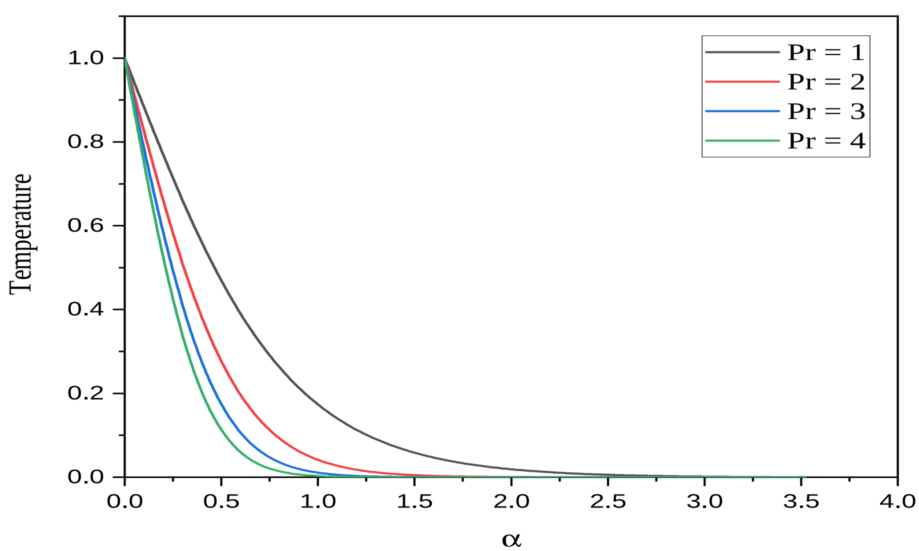

FIGURE 15. Temperature versus α for $m = 1.2$, $\overline{\beta} = 0.5$ and $\sigma = 2$

REFERENCES

1. Abel, M. S., & Nandeppanavar, M. M. (2007). Effects of thermal radiation and non-uniform heat source on MHD flow of viscoelastic fluid and heat transfer over a stretching sheet. International Journal of Applied Mechanics and Engineering, 12(4), 903-918. https://doi.org/10.1016/j.apm.2007.06.038
2. Achala, L. N. & Asha, C.S. (2015). Analysis of flow of polar and non polar incompressible ferrofluids, *Journal of Advances in Physics*, Vol. 10, No. 2, 2733-2740. https://doi.org/10.1007/s10973-020-09636-5
3. Adnan, Khan, U., Ahmed, N., Manzoor, R., & Mohyud-Din, S. T. (2021). Impacts of various shaped Cu-nanomaterial on the heat transfer over a bilateral stretchable surface: Numerical investigation. Advances in Mechanical Engineering, 13(12), 16878140211067420. https://doi.org/10.1177/16878140211067420
4. Asha C. S., & Achala L. N., (2017), Study of magnetoviscosity and spin velocity of a ferrofluid flow between inclined planes. International Journal of Latest Trends in Engineering and Technology, Vol. 9, No. 1, 14-21. http://dx.doi.org/10.21172/1.91.03
5. Bhandari, A. (2021). Water-based ferrofluid flow and heat transfer over a stretchable rotating disk under the influence of an alternating magnetic field. Proceedings of the Institution of Mechanical Engineers, Part C: Journal of Mechanical Engineering Science, 235(12), 2201-2214. https://doi.org/10.1177/0954406220952515
6. Cochran, W. G. (1934). The Flow Due to a Rotating Disk. Mathematical Proceedings of the Cambridge Philosophical Society, Vol. 30, No. 3, 365-375. https://doi.org/10.1017/S0305004100012561
7. Crane, L. J. (1970). Flow past a stretching plate. Zeitschrift für angewandte Mathematik und Physik ZAMP, 21, 645-647. https://doi.org/10.1007/BF01587695
8. Das, K. (2015). Nanofluid flow over a non-linear permeable stretching sheet with partial slip. Journal of the Egyptian mathematical society, 23(2), 451-456. https://doi.org/10.1016/j.joems.2014.06.014
9. Ellahi, R., Tariq, M. H., Hassan, M., & Vafai, K. (2017). On boundary layer nano-ferroliquid flow under the influence of low oscillating stretchable rotating disk. Journal of Molecular Liquids, 229, 339-345. https://doi.org/10.1016/j.molliq.2016.12.073
10. Fang, T. (2007). Flow over a stretchable disk. Physics of fluids. Vol.19, No. 12, 128105. https://doi.org/10.1063/1.2823572
11. Hassan, M., Fetecau, C., Majeed, A., & Zeeshan, A. (2018). Effects of iron nanoparticles' shape on convective flow of ferrofluid under highly oscillating magnetic field over stretchable rotating disk. Journal of Magnetism and Magnetic Materials, 465, 531-539. https://doi.org/10.1016/j.jmmm.2018.06.019
12. Joshi, V. K., Ram, P., Tripathi, D., & Sharma, K. (2018). Numerical investigation of magnetic nanofluids flow over rotating disk embedded in a porous medium. Thermal Science, 22(6 Part B), 2883-2895. https://doi.org/10.2298/TSCI170323139J
13. Karman, V.(1972). Uber laminare and turbulente Reibung, Zeitschrift für Angewandte Mathematik und Mechanik, Vol. 1, No. 4, 1921, 232-252. https://doi.org/10.1002/zamm.19210010401
14. Mitamura, Y., Wada, T., & Sakai, R. (1992). A ferrofluidic actuator for an implantable artificial heart. Artificial Organs, 16(5), 490-495. https://doi.org/10.1111/j.1525-1594.1992.tb00329.x
15. Nandeppanavar, M. M., Prasannakumara, B. C., & Shilpa, J. M. (2018). Three-dimensional flow, heat and mass transfer of MHD non-newtonian nanofluid due to stretching sheet. Journal of Nanofluids, 7(4), 635-645. https://doi.org/10.1166/jon.2018.1498
16. Nandeppanavar, M. M., Vajravelu, K., & Datti, P. S. (2016). Optimal homotopy asymptotic solutions for nonlinear ordinary differential equations arising in flow and heat transfer due to nonlinear stretching sheet. Heat Transfer—Asian Research, 45(1), 15-29. https://doi.org/10.1002/htj.21149

17. Nandeppanavar, M. M., Abel, M. S., & Kemparaju, M. C. (2017). Stagnation point flow, heat and mass transfer of MHD nanofluid due to porous stretching sheet through porous media with effect of thermal radiation. Journal of Nanofluids, 6(1), 38-47. https://doi.org/10.1016/j.csite.2023.103345
18. Nanjundappa, C. E., Shivakumara, I. S., & Lee, J. (2014). Effect of Coriolis Force on Bénard–Marangoni Convection in a Rotating Ferrofluid Layer with MFD Viscosity. Microgravity Science and Technology, Vol. 27, No. 1, 27–37. https://doi.org/10.1007/s12217-014-9410-0
19. Pal, D. (2009). Heat and mass transfer in stagnation-point flow towards a stretching surface in the presence of buoyancy force and thermal radiation. Meccanica, 44(2), 145-158. https://doi.org/10.1007/s11012-008-9155-1
20. Priyadharshini, P., & Karpagam, V. (2024). Machine learning impact of radiative blood flow over a wedge in a time-dependent MHD Williamson fluid. Annals of Mathematics and Computer Science, 22, 12-44. https://doi.org/10.56947/amcs.v22.275
21. Raj, K., and Moskowitz, R. (1990). Commercial applications of ferrofluids. Journal of Magnetism and Magnetic Materials, 85(1-3), 233-245. https://doi.org/10.1016/0304-8853(90)90058-X
22. Ram, P., Bhandari, A., & Sharma, K. (2010). Effect of magnetic field-dependent viscosity on revolving ferrofluid. Journal of Magnetism and Magnetic Materials, Vol.322, No.21, 3476–3480. https://doi.org/10.1016/j.jmmm.2010.06.048
23. Ram, P., & Sharma, K. (2011). Revolving Ferrofluid Flow under the Influence of MFD Viscosity and Porosity with Rotating Disk. Journal of Electromagnetic Analysis and Applications, Vol.3, No.9, , Article ID:7463. https://doi.org10.4236/jemaa.2011.39060
24. Ram, P., & Kumar, V. (2013). FHD flow with heat transfer over a stretchable rotating disk. Multidiscipline Modeling in Materials and Structures, Vol. 9, No. 4, 524-537. https://doi.org/10.1108/MMMS-03-2013-0013
25. Ram, P. & Kumar, V. (2012). Ferrofluid Flow With Magnetic Field-Dependent Viscosity due to Rotating Disk in Porous Medium. International Journal of Applied Mechanics, Vol.04, No.4, 1250041. https://doi.org/10.1142/S175882511250041X
26. Ram, P., Joshi, V. K., Sharma, S., & Yadav, N. (2018). Boundary layer flow of magnetic nanoliquids due to a radially rotating stretchable plate. In Materials Science Forum (Vol. 928, pp. 100-105). Trans Tech Publications Ltd. https://doi.org/10.4028/www.scientific.net/msf.928.100.
27. Rana, P., & Bhargava, R. (2012). Flow and heat transfer of a nanofluid over a nonlinearly stretching sheet: a numerical study. Communications in Nonlinear Science and Numerical Simulation, 17(1), 212-226. https://doi.org/10.1016/j.cnsns.2011.05.009
28. Rosensweig, R. E. (1966). Buoyancy and stable levitation of a magnetic body immersed in a magnetizable fluid. Nature, 210(5036), 613-614. https://doi.org/10.1038/210613a0
29. Rosensweig, R. E., *Ferrohydrodynamics*, Dover Publications, Cambridge University Press,1985. https://books.google.co.in/books/about/Ferrohydrodynamics.html?id=s7QmAgAAQBAJ&source=kp_book_description&redir_esc=y
30. Sakiadis, B. C. (1961). Boundary-layer behavior on continuous solid surfaces: II. The boundary layer on a continuous flat surface. AiChE journal, 7(2), 221-225. https://doi.org/10.1002/aic.690070211
31. Samad Khan, A., Abrar, M. N., Uddin, S., Awais, M., & Usman, I. (2022). Entropy generation due to micro-rotating Casson's nanofluid flow over a nonlinear stretching plate: Numerical treatment. Waves in Random and Complex Media, 1-16. https://doi.org/10.1080/17455030.2022.2067376
32. Sandeep, N., Kumar, B. R., & Kumar, M. J. (2015). A comparative study of convective heat and mass transfer in non-Newtonian nanofluid flow past a permeable stretching sheet. Journal of Molecular Liquids, 212, 585-591. https://doi.org/10.1016/j.molliq.2015.10.010

33. Shamshuddin, M. D., Abderrahmane, A., Koulali, A., Eid, M. R., Shahzad, F., & Jamshed, W. (2021). Thermal and solutal performance of Cu/CuO nanoparticles on a non-linear radially stretching surface with heat source/sink and varying chemical reaction effects. International Communications in Heat and Mass Transfer, 129, 105710. https://doi.org/10.1016/j.icheatmasstransfer.2021.105710
34. Sharma, K., & Kumar, S. (2023). Impacts of low oscillating magnetic field on ferrofluid flow over upward/downward moving rotating disk with effects of nanoparticle diameter and nanolayer. Journal of Magnetism and Magnetic Materials, 575, 170720. https://doi.org/10.1016/j.jmmm.2023.170720
35. Sharma, R., Ishak, A., & Pop, I. (2014). Stability analysis of magnetohydrodynamic stagnation-point flow toward a stretching/shrinking sheet. Computers and Fluids, 102, 94-98. https://doi.org/10.1016/j.compfluid.2014.06.022
36. Sheikholeslami, M., Mustafa, M. T., & Ganji, D. D. (2015). Nanofluid flow and heat transfer over a stretching porous cylinder considering thermal radiation. Iranian Journal of Science and Technology (Sciences), 39(3.1), 433-440. 10.22099/IJSTS.2015.3267
37. Sheikholeslami, M., & Shehzad, S. A. (2018). Numerical analysis of $Fe3O4–H2O$ nanofluid flow in permeable media under the effect of external magnetic source. International Journal of Heat and Mass Transfer, 118, 182-192. https://doi.org/10.1016/j.ijheatmasstransfer.2017.10.113
38. Shliomis, M. I., & Morozov, K. I. (1994). Negative viscosity of ferrofluid under alternating magnetic field. Physics of Fluids, 6(8), 2855-2861. https://doi.org/10.1063/1.868108
39. Shokrollahi, H. (2013). Structure, synthetic methods, magnetic properties and biomedical applications of ferrofluids. Materials Science and Engineering: C, 33(5), 2476-2487. https://doi.org/10.1016/j.msec.2013.03.028
40. Siddheshwar, P. G., & Mahabaleswar, U. S. (2005). Effects of radiation and heat source on MHD flow of a viscoelastic liquid and heat transfer over a stretching sheet. International Journal of Non-Linear Mechanics, 40(6), 807-820. https://doi.org/10.1016/j.ijnonlinmec.2004.04.006
41. Sil, S. (2024). Flow of MHD micropolar fluid through porous medium: a hodograhic approach for exact solution. Annals of Mathematics and Computer Science, 22, 128-148. https://doi.org/10.56947/amcs.v22.287
42. Sulochana, C., Ashwinkumar, G. P., & Sandeep, N. (2016). Transpiration effect on stagnation-point flow of a Carreau nanofluid in the presence of thermophoresis and Brownian motion. Alexandria Engineering Journal, 55(2), 1151-1157. https://doi.org/10.1016/j.aej.2016.03.031
43. Sunil, Sharma, A., & Shandil, R. G., (2008). Effect of magnetic field dependent viscosity on ferroconvection in the presence of dust particles. Journal of Applied Mathematics and Computing, Vol.27, No. 1-2, 7–22. https://doi.org/10.1007/s12190-008-0055-2
44. Tripathy, R. S., Dash, G. C., Mishra, S. R., & Hoque, M. M. (2016). Numerical analysis of hydromagnetic micropolar fluid along a stretching sheet embedded in porous medium with non-uniform heat source and chemical reaction. Engineering science and technology, an international journal, 19(3), 1573-1581. https://doi.org/10.1016/j.jestch.2016.05.012
45. Thirupathi, G., & Singh, R. (2014). Magneto-viscosity of MnZn-ferrite ferrofluid. Physica B: Condensed Matter, 448, 346-348. https://doi.org/10.1016/j.physb.2014.03.042
46. Turkyilmazoglu, M. (2012). MHD fluid flow and heat transfer due to a stretching rotating disk. International journal of thermal sciences, Vol.51, 195-201. https://doi.org/10.1016/j.ijthermalsci.2011.08.016
47. Vaidyanathan, G., Sekar, R., Vasanthakumari, R., & Ramanathan, A. (2002). The effect of magnetic field dependent viscosity on ferroconvection in a rotating sparsely distributed porous medium. Journal of Magnetism and Magnetic materials, 250, 65-76. https://doi.org/10.1016/S0304-8853(02)00355-4
48. Varun Kumar, R. S., Alhadhrami, A., Punith Gowda, R. J., Naveen Kumar, R., & Prasannakumara, B. C. (2021). Exploration of Arrhenius activation energy on hybrid nanofluid flow over

a curved stretchable surface. ZAMM-Journal of Applied Mathematics and Mechanics/Zeitschrift für Angewandte Mathematik und Mechanik, 101(12), e202100035. https://doi.org/10.1002/zamm.202100035

49. Varun Kumar, R. S., Gunderi Dhananjaya, P., Naveen Kumar, R., Punith Gowda, R. J., & Prasannakumara, B. C. (2022). Modeling and theoretical investigation on Casson nanofluid flow over a curved stretching surface with the influence of magnetic field and chemical reaction. International Journal for Computational Methods in Engineering Science and Mechanics, 23(1), 12-19. https://doi.org/10.1080/15502287.2021.1900451
50. Yang, W., Zhang, Y., Yang, X., Sun, C., & Chen, Y. (2022). Systematic analysis of ferrofluid: a visualization review, advances engineering applications, and challenges. Journal of Nanoparticle Research, 24(6), 102. https://doi.org/10.1007/s11051-022-05477-5

[1,2,3,4] P.G. Department of Mathematics and Research Centre in Applied Mathematics, M E S College of Arts, Commerce and Science, 15th cross, Malleswaram, Bengaluru-560003, India.
Email address: [1]meghashree01@gmail.com
Email address: [2]csasharukmini@gmail.com
Email address: [3]sumana.shesha@gmail.com
Email address: [4]anargund1960@gmail.com

[5,6] Department of Mathematics, National Institute of Technology, Chaltlang, Aizawl - 796012, Mizoram, India.
Email address: [5]laxmirathour817@gmail.com
Email address: [6]vinaysingh14aug@gmail.com

[7] Department of Mathematics, School of Advanced Sciences, Vellore Institute of Technology, Vellore - 632014, Tamil Nadu, India.
Email address: lakshminarayanmishra04@gmail.com

[8] Department of Mathematics, Indira Gandhi National Tribal University, Lalpur, Amarkantak, Anuppur - 484887, Madhya Pradesh, India.
Email address: vishnunarayanmishra@gmail.com